

# THE 4TH INTERNATIONAL CONFERENCE ON ALUMINUM ALLOYS

## FORMABILITY OF ALUMINUM 2024-O SHEET\*

K. G. Anand, V. Ramnarayan and P. K. Chaudhury  
Concurrent Technologies Corporation  
Johnstown, PA 15904

### Abstract

Formability of materials during sheetmetal forming is limited by strain localization. In addition to experimental methods, numerical techniques are used to predict the formability of sheet materials. This work focuses on finite element simulation (FEM) of limiting dome height (LDH) tests, and experimental determination of strain contours for comparison with FEM predictions. The strain contours were determined by accurately measuring digitized grid deformations in LDH samples. Finite element simulations were performed using the general purpose commercial code, ABAQUS1. Numerical results have been compared with experimental data obtained from the LDH tests for Aluminum Alloy 2024-O. Good correspondence was found between strain distributions predicted by FEM and those calculated from measurements made on test samples.

### Introduction

The usual means of assessing sheet formability is through the standard tension test to measure elongation of materials, or by stretching fully clamped sheets to failure in hemispherical punch tests. The latter is a simple, quick and reliable experimental method for the determination of the forming limit diagram (FLD) proposed by Hecker<sup>2</sup>. Ghosh<sup>3</sup> proposed that the height of the dome at maximum load can be used as a measure of formability for sheet materials. Using specimens with various width-to-length ratios to obtain different minor-to-major strain ratios during testing, Ghosh demonstrated that the LDH curve corresponds closely with the FLD for the material. However, considerable difficulties are encountered in making measurements on deformed samples.

Several mathematical models have been developed to predict the FLD<sup>4,5</sup>. For the biaxial stretching analysis, Marciniak and Kuczynski (MK) postulated that localized necking initiates from a pre-existing material imperfection<sup>4</sup>. This imperfection can be represented as a linear groove lying parallel to the minor strain direction. A principal objection to this theory is that predicted results are extremely sensitive to the imperfection factor, which is difficult to quantify<sup>5,6</sup>. Jones and Gillis (JG) have proposed a plastic deformation model based on features observed from a tensile test<sup>5</sup>. Whereas analytical models use Hill's quadratic flow criterion<sup>7</sup>, which has only four constants to incorporate experimentally measured quantities, the flow rule proposed by Jones and

---

\* This work was performed by the National Center for Excellence in Metalworking Technology, operated by Concurrent Technologies Corporation, under contract to the U. S. Navy as part of the U. S. Navy Manufacturing Technology Program.

Gillis can incorporate six experimentally measured quantities, which results in better predictions of material forming limits.

Finite element (FE) methods present another avenue for obtaining predictions of material forming limits and other important information such as strain distribution and strain paths in various regions of the workpiece. However, considerable time is invested in developing FE models to predict metal deformation, and further development is usually necessary to simulate the forming of complex shapes. Experimental information is often necessary to verify FE predictions. Hence, there is a need for a reliable, accurate and quick experimental method to measure grid deformations in sheet components with both simple and complex shapes. Such an experimental method can also serve as a verification tool for FE simulations of sheet forming processes. A measurement technique has been developed in which grid deformations are digitized and accurately measured and efforts are presently underway to automate this technique.

Finite element simulations of the limiting dome height tests were performed for two specimens with different width-to-length ratios. The LDH test was performed on samples with various width-to-length ratios and the principal strains were calculated along the width and length dimensions of the samples. This paper focuses on comparison of strain contours predicted by FE simulations and those determined experimentally. Additionally, the limiting dome height curve for the alloy is presented to obtain a measure of forming limits in the material.

### Experimental Procedure

#### Tension Test

Uniaxial tension tests were performed to obtain the directional material properties for the finite element simulation of the LDH test. These tests were performed at room temperature and at a constant cross-head speed (0.3 in./min.) using tensile dog-bone specimens at orientations from 0 to 90 degrees between the tensile axis and the rolling direction at 22.5 degree intervals. The gage length of the specimens used in the experiments was 1.25 inches, and the specimens were 0.25 inches wide and 0.06 inches thick. A square grid pattern of dimension 0.05 inch was machined on the specimen surfaces. The tests were performed to evaluate the directional properties which include tensile strength ( $\sigma_U$ ), strain hardening coefficient ( $n$ ), plastic strain ratio ( $R$ =ratio of width to thickness strain) and the percentage elongation to failure.  $R$  values were determined at 15% tensile elongation.

#### LDH Test

Test specimens with different width-to-length ratios and 0.06 inch in thickness were machined from Al 2024-O sheet to provide different strain paths to failure during LDH testing. To facilitate calculation of the limiting major and minor strains after testing, square grids measuring 0.05 in. in length were machined on the surface of the specimens. The sheet specimens were stretched to failure at room temperature by a hemispherical punch in a Tinius-Olsen Ductomatic sheet tester. No lubrication was applied to the test specimens. The diameter of the punch used in the tests was 2.7 inches and the sheet specimens were deformed at a constant velocity of 0.3 in./min. until failure, which was indicated by a sudden drop in the load. Approximately 3000 lb clamping force was applied to prevent drawing-in of material from the width direction during testing. Data were acquired on the ram load and displacement. The details on the LDH setup are given elsewhere<sup>8</sup>. Major and minor strains of the specimen after LDH testing were measured by using an optical grid analyzer. Displacement measurements in the grids adjacent to the crack were used to calculate the limiting strains used to develop the LDH curve.

#### Finite Element Simulation of the LDH Test

The finite element model for limiting dome height test simulation was developed using ABAQUS S4R shell elements. This is a four-node, reduced integration, doubly curved shell element with hourglass control. This element enables the calculation of the elastic as well as plastic behavior of the material, and takes into account through-thickness effects. Hence, springback and bending effects could be handled in a more accurate manner. Anisotropic material behavior was incorporated into the models. The punch was modeled as a rigid surface, and contact elements

(interface element type IRS13) connected each node on the contact area between the punch and the workpiece. Coulomb friction was used to characterize sliding ( $\mu=0.3$ ) friction conditions. Nodes at the edge of the mesh which correspond to the region between the clamping dies are fully constrained so that no drawing-in of the material between the dies occurs. The punch diameter used for developing the finite element model was 2.70 inches and the circular blank diameter was 4.0 inches. The punch was moved using displacement control. Strain rate effects were not considered in these simulations. Since a fracture criterion was not incorporated in these simulations, experimentally measured dome heights at failure were used to obtain predictions of strain distributions in FE simulations of the LDH test.

### Results and Discussions

#### Tensile Properties

The results of uniaxial tensile test are summarized in Table I. The stress strain curves obtained from tensile tests are shown in Figure 2. The strain hardening exponent values range from 0.31 to 0.4 and the ultimate stress values range from 166.2 MPa to 180 MPa. The material also exhibits similar elongation values along the various orientations. The plastic strain ratio values indicate that the material is isotropic. The strain hardening exponent, tensile strength and elongation values from Table I further strengthen this observation of isotropic behavior.

TABLE I: TENSILE TEST RESULTS

Orientation	0 (deg)	22.5 (deg)	45	67.5	90
$\sigma_U$ (MPa)	180	174.5	166.9	166.2	169.6
R	0.92	0.94	0.93	0.88	0.95
n	0.40	0.31	0.33	0.37	0.38
% Elongation	23.7	25.3	26.9	24.2	24.4

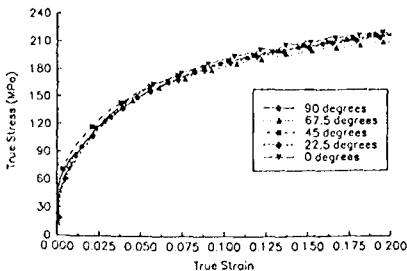


Figure 2 Stress-strain curves for Al alloy 2024

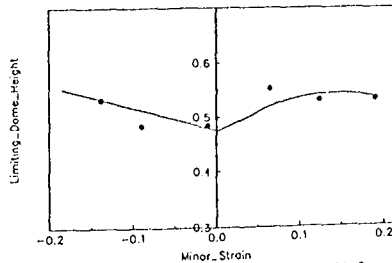


Figure 3 Limiting Dome Height curve for Al2024-O

#### LDH Tests

In the LDH experiments, the clamped sheets were deformed to failure by pushing a 68.58 mm (2.7 inch) diameter hemispherical punch against the sheets. The dome heights at failure were measured and normalized with respect to the punch radius to obtain the limiting dome height (LDH) values. These LDH values were plotted against the critical minor strain calculated from grid deformations measured in the vicinity of the crack. The LDH curve for aluminum alloy 2024-O is shown in Figure 3. The minimum value ( $LDH_0$ ) representing plane strain deformation is at 0.475 on the ordinate. The LDH curve is representative of the FLD for the material.

Grid deformations to a distance of one inch on either side of the pole of the specimens were measured along a line transverse to the crack. Figures 4 and 5 represent the major strain distribution values calculated from the grid distortions for the partial width (50 mm) and full dome (100 mm) specimens, respectively. Stereo photography was used to obtain enlarged pictures, after deformation, of the grids scribed on the surface of the sheet. The magnification factor used in the

current work was 6.7. The grids were digitized on a precision digitizing tablet of 20  $\mu\text{m}$  resolution. A cubic spline was fitted to the displaced grid to obtain the slope of the curve at the grid points from which in-plane displacements and strains were calculated. Statistical analysis was performed to determine the error in strain calculations. The error calculated was of the order of 0.4%.

The LDH tests for specimens with widths corresponding to 50 mm and 100 mm were simulated using the finite element method (FEM) to obtain the deformation profile and strain distribution. Since these simulations did not incorporate a failure criterion, dome heights at failure measured on experimental LDH test samples were used to obtain predictions of major and minor strain values. Figures 6 through 9 present the examples of FEM simulation of the LDH test specimens for the width-to-length ratios mentioned above. The gray scale indicates the strain severity in the deformed specimen.

### Comparison of Numerical Predictions and Experimental Results

Figures 4 and 5 represent the major and minor strain contour plots obtained from measurements of grid distortions along lines transverse to the crack. The ordinate represents the distance from the pole of the specimen (in mm.) while the abscissa represents the grid location from the approximate center of the fracture line. The strain contour plots show concentrations approximately 12 mm from the pole in both specimens, the region of failure in the specimens. A high major strain value (approximately 1.0) is measured in this area, and is due to separation of material along the fracture line. The LDH curve from Figure 2 indicates that typical major strain values are 0.55 for the sample widths in consideration.

Figures 6 and 8 represent the displaced mesh geometries while 7 and 9 represent the major strain contour predictions from FE simulations for the partial width and full dome specimens, respectively. In these figures, the 1 direction corresponds to the width direction while 2 corresponds to the length direction.

The FEM simulations predict a trend similar to those observed from experiments. Major strain values closely matching experimental values in the vicinity of the fracture area in test specimens are predicted. However, FE predictions indicate strain concentrations in regions different from those observed in test specimens. FE analyses predict failure 20-25mm away from the pole of the specimen in the partial width and full dome specimens. A reason for this may be the low friction factor used in the simulations. Higher friction values will produce strain concentrations in the unsupported regions of the sheet. Strain values of 0.572 and 0.559 are predicted in the two samples at these locations which correspond well with measured values at fracture locations. Hence, good correspondence is obtained between experimental results and predicted values.

### Conclusion

The experimental forming limits of Al 2024-O sheets were determined by performing LDH tests. A reliable method has been developed to digitally measure grid deformations in test samples. Simplified finite element simulations of the LDH test were performed and compared with experimental data. Good agreement was obtained between predicted and experimental strain profiles and maximum strain values at locations corresponding to fracture sites in experimental samples.

### References

1. ABAQUS is a trade name of Hibbitt, Karlsson and Sorenson, Inc., Rhode Island.
2. S. S. Hecker, Sheet Metal Industries, November, p. 671 (1975).
3. A. K. Ghosh, Metals Engineering Quarterly, August, p. 53 (1975).
4. Z. Marciniak and K. Kuczynski, Int. J. Mech. Sci., Vol. 9, p. 609 (1967).
5. W. Choi, P. P. Gillis, and S. E. Jones, Metall. Trans. A, Vol. 20A, p. 1975 (1989).
6. A. Graf, and W. F. Hosford, Metall. Trans. A, V. 21A, p. 87 (1990).
7. R. Hill, Proc. Roy. Soc., V. A193, p. 281 (1948).
8. C. J. Yu, K. G. Anand, V. Ramnarayan, K. C. Wang and P. K. Chaudhury, Proc. 3rd Int. SAMPE Metals Processing Conference, pp. M242-M252, 1992.

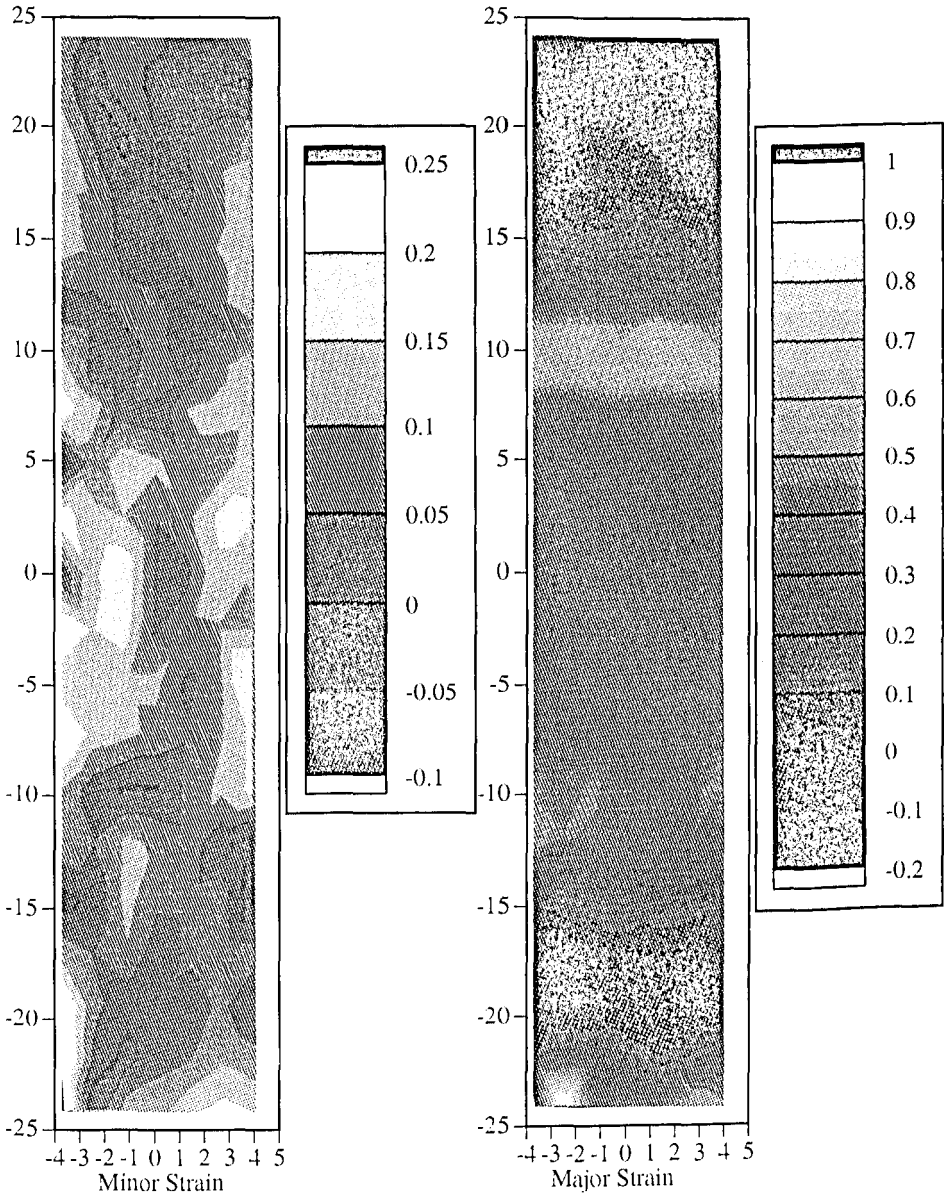


Figure 4 Strain contours in a partial width (50 mm) sample

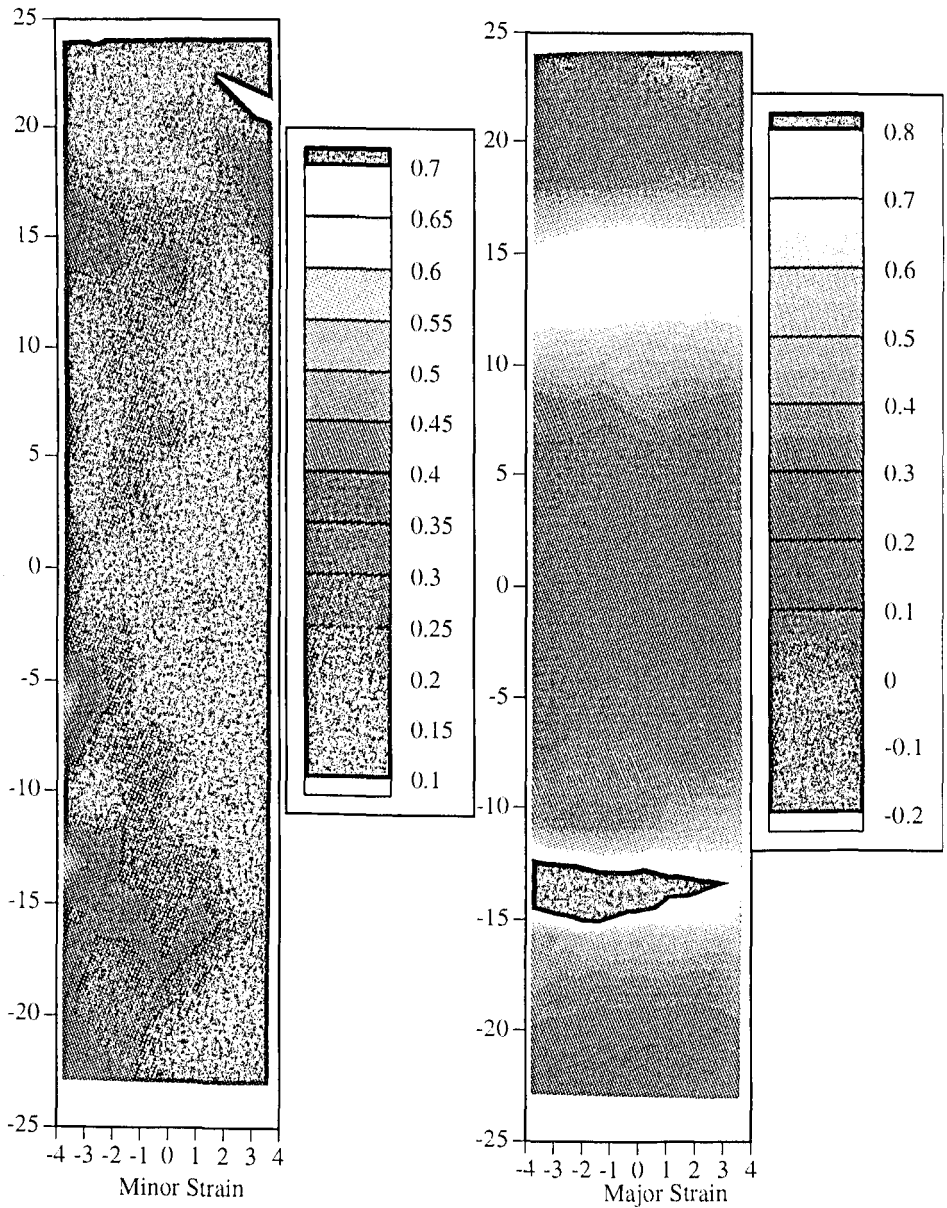


Figure 5 Strain contours in a full dome (100 mm) sample

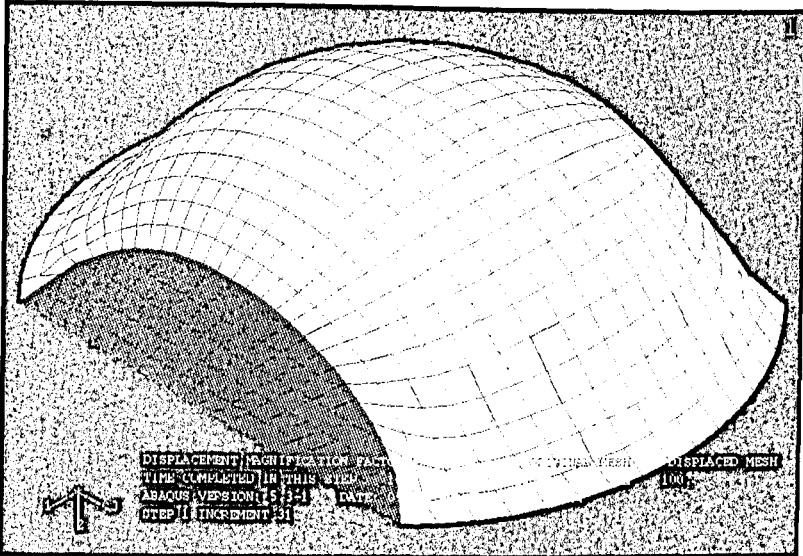


Figure 6 Displaced mesh geometry for 50mm width specimen

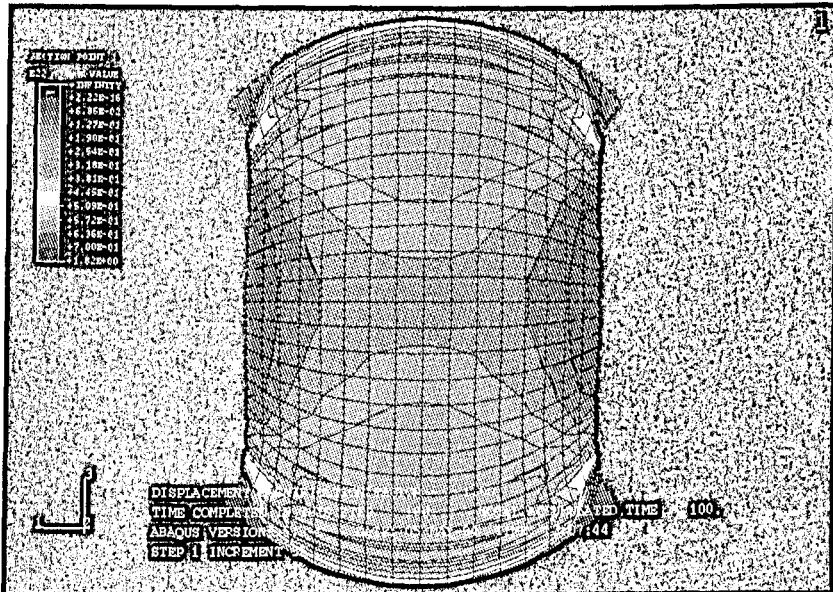


Figure 7 Major strain distribution for 50 mm width specimen

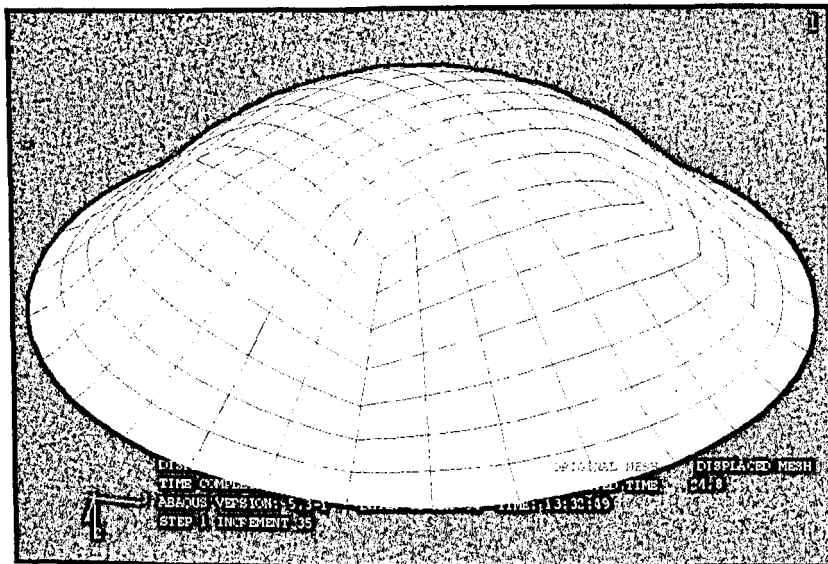


Figure 8 Displaced mesh geometry for full dome specimen

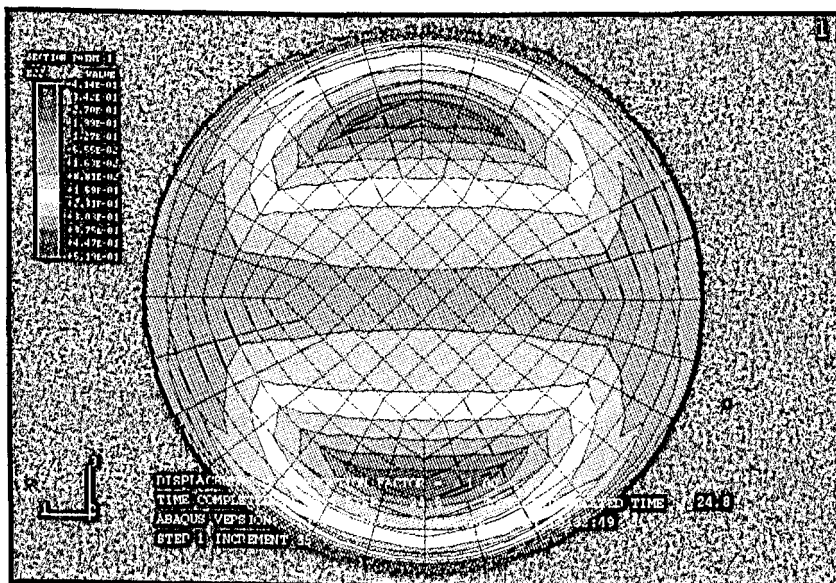


Figure 9 Major strain distribution for full dome specimen